ISSN 1070-3284, Russian Journal of Coordination Chemistry, 2020, Vol. 46, No. 4, pp. 251–259. © Pleiades Publishing, Ltd., 2020.
Russian Text © The Author(s), 2020, published in Koordinatsionnaya Khimiya, 2020, Vol. 46, No. 4, pp. 232–240.

Photoluminescence of the Coordination Zinc Compounds with 3-Methyl-4-Formyl-1-Phenylpyrazol-5-one Acylhydrazones

A. N. Gusev[a], *, E. V. Braga[a], M. A. Kryukova[b], N. V. Lyubomirskii[a], E. A. Zamnius[a], and V. F. Shul'gin[a]

[a] *Vernadsky Federal University, Simferopol, Crimea, Russia*

[b] *St. Petersburg State University, St. Petersburg, 199164 Russia*

**e-mail: galex0330@rambler.ru*

Received October 20, 2019; revised November 12, 2019; accepted November 15, 2019

Abstract—New coordination zinc compounds based on 3-methyl-4-formyl-1-phenylpyrazol-5-one acylhydrazones [Zn(L)(CH_3COO)Solv] (Solv is H_2O (**I**), Py (**II**)) are synthesized in order to search for new luminophores demonstrating efficient photoluminescence in the visible range. Complexes **I** and **II** are characterized by elemental and thermogravimetric analyses, mass spectrometry, and UV and IR spectroscopy. The structures of two complexes [$Zn(L^5)(CH_3COO)H_2O$] and [$ZnL^4(CH_3COO)Py$] are determined by X-ray structure analysis (CIF files CCDC nos. 1958400 and 1958401, respectively). Complexes **I** and **II** demonstrate luminescence in the visible range with a maximum at 414–536 nm and a quantum yield of 9.5–64% depending on the nature of the acyl fragment.

Keywords: photoluminescence, zinc complexes, hydrazones

DOI: 10.1134/S107032842004003X

INTRODUCTION

In the recent decades, the coordination zinc compounds exhibiting the luminescence properties attract increasing attention of researchers as an alternative to more expensive luminophores based on the complexes of platinum metals [1] and lanthanides [2]. The fully filled *d* shell of the zinc cation results in the occurrence of only intraligand π–π* transitions during luminescence [3, 4]. Therefore, the main factor that allows one to control the photophysical characteristics of the zinc complexes is the optimum design of the corresponding organic ligands. The complexes with the ligands containing the donor oxygen and nitrogen atoms and conjugated aromatic fragments are most abundant [5–7]. These compounds demonstrate the high luminous parameters and also are promising sources of the blue radiation, which is necessary for the production of full-color electroluminescent devices. Nevertheless, only several types of organic derivatives, whose coordination compounds demonstrate the optical properties perspective for practical use, have been described. The best parameters were obtained for the azomethine derivatives of salicylaldehyde and its heterocyclic analogs [8–11]. However, the use of acylhydrazones as an organic matrix is presented by single examples. Only the available published data show the high fluorescence efficiency and thermal stability [12–14]. It should be mentioned that the main attention is given to hydrazones based on salicylaldehyde and its analogs and, hence, it seems promising to search for alternative ligands capable of efficiently binding zinc cations and demonstrating photoluminescence in the visible range [15].

The results of the study of the structures and photoluminescence properties of the coordination zinc compounds with hydrazones of 3-methyl-4-formyl-1-phenylpyrazol-5-one and some carboxylic acids are presented in this report.

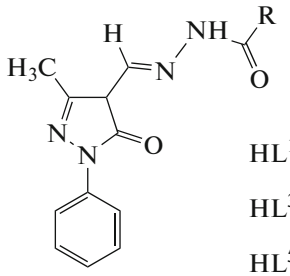

HL^1: R = C_6H_5 HL^2: R = *p*-$CH_3C_6H_4$

HL^3: R = *p*-$CH_3OC_6H_4$ HL^4: R = *p*-ClC_6H_4

HL^5: R = $C_6H_5CH_2$ HL^6: R = $C_6H_5CH_2CH_2$

EXPERIMENTAL

Zinc acetate dihydrate (analytical grade) served as the initial compound. 3-Methyl-4-formyl-1-phenylpyrazol-5-one was synthesized using the modified procedure [16]. Hydrazones HL^1–HL^6 were synthesized according to previously described procedures [17]. The solvents used in the work (ethanol, acetonitrile, and pyridine) were preliminarily purified by distillation.

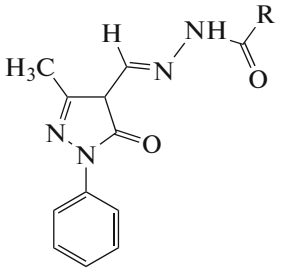

+ $Zn(CH_3COO)_2 \cdot 2H_2O \xrightarrow[EtOH/Py]{EtOH/H_2O}$ $ZnL(CH_3COO)H_2O$ **I–VI**; $ZnL(CH_3COO)Py$ **VII–XII**

Synthesis of coordination compounds I–VI. 3-Methyl-4-formyl-1-phenylpyrazol-5-one (2 mmol) was dissolved in 96% ethanol (25 mL) with stirring on heating (50–60°C), and the corresponding hydrazide (2 mmol) was added to the obtained solution. A precipitate was formed during further stirring and heating for 1–2 h, and ethanol (10 mL) and $Zn(OAc)_2 \cdot 2H_2O$ (2 mmol) were added to the precipitate. The reaction mixture was stirred on heating with a reflux condenser for 4 h. The formed precipitate was left to stay overnight above the mother liquor and then was filtered off, washed with ethanol, and dried in air. Complexes **I**–**VI** were obtained.

Complex $[Zn(L^1)(CH_3COO)H_2O]$ (**I**), acetato-*N*'-(3-methyl-5-oxy-1-phenylpyrazol-4-yl)methylene]benzohydrazidozinc hydrate, was formed as light yellow crystals in a yield of 72%. IR (ν, cm^{-1}): 1596 (Amide-I), 1554 (COO^-), 1530 (C=N), 1354 (COO^-), 1339 (C_{pyr}–O).

For $C_{20}H_{22}N_4O_6Zn$

Anal. calcd., %	C, 50.06	H, 4.62	N, 11.67
Found, %	C, 49.91	H, 4.66	N, 11.64

Complex $[Zn(L^2)(CH_3COO)H_2O]$ (**II**), acetato-*N*'-(3-methyl-5-oxy-1-phenylpyrazol-4-yl)methylene]-4-methylbenzohydrazidozinc hydrate, was formed as light yellow crystals in a yield of 59%. IR (ν, cm^{-1}): 1596 (Amide-I), 1559 (COO^-), 1528 (C=N), 1358 (COO^-), 1340 (C_{pyr}–O).

For $C_{21}H_{22}N_4O_5Zn$

Anal. calcd., %	C, 53.05	H, 4.63	N, 11.79
Found, %	C, 53.21	H, 4.84	N, 11.91

Complex $[Zn(L^3)(CH_3COO)H_2O]$ (**III**), acetato-*N*'-(3-methyl-5-oxy-1-phenylpyrazol-4-yl)methylene]-4-methoxybenzohydrazidozinc hydrate, was formed as light yellow crystals in a yield of 86%. IR (ν, cm^{-1}): 1601 (Amide-I), 1558 (COO^-), 1528 (C=N), 1348 (COO^-), 1343 (C_{pyr}–O).

For $C_{21}H_{22}N_4O_6Zn$

Anal. calcd., %	C, 51.32	H, 4.48	N, 11.41
Found, %	C, 51.27	H, 4.30	N, 11.28

Complex $[Zn(L^4)(CH_3COO)H_2O]$ (**IV**), acetato-*N*'-(3-methyl-5-oxy-1-phenylpyrazol-4-yl)methylene]-4-chlorobenzohydrazidozinc hydrate, was formed as light yellow crystals in a yield of 78%. IR (ν, cm^{-1}): 1595 (Amide-I), 1566 (COO^-), 1526 (C=N), 1362 (COO^-), 1343 (C_{pyr}–O).

For $C_{20}H_{19}N_4O_5ClZn$

Anal. calcd., %	C, 48.48	H, 3.83	N, 11.30
Found, %	C, 48.29	H, 4.06	N, 11.29

Complex $[Zn(L^5)(CH_3COO)H_2O]$ (**V**), acetato-*N*'-(3-methyl-5-oxy-1-phenylpyrazol-4-yl)methylene]-2-phenylethanohydrazidozinc hydrate, was formed as cream-colored crystals in a yield of 63%. IR (ν, cm^{-1}): 1606 (Amide-I), 1562 (COO^-), 1530 (C=N), 1353 (COO^-), 1346 (C_{pyr}–O).

For $C_{21}H_{22}N_4O_5Zn$

Anal. calcd., %	C, 53.05	H, 4.63	N, 11.79
Found, %	C, 53.16	H, 4.31	N, 11.65

Complex $[Zn(L^6)(CH_3COO)H_2O]$ (**VI**), acetato-*N*'-(3-methyl-5-oxy-1-phenylpyrazol-4-yl)methylene]-3-phenylpropanohydrazidozinc hydrate, was formed as cream-colored crystals in a yield of 78%. IR (ν, cm^{-1}):

1607 (Amide-I), 1560 (COO^-), 1529 (C=N), 1361 (COO^-), 1346 (C_{pyr}–O).

For $C_{22}H_{24}N_4O_5Zn$

Anal. calcd., %	C, 53.94	H, 4.94	N, 11.44
Found, %	C, 53.78	H, 5.17	N, 11.52

Synthesis of coordination compounds VII–XII. 3-Methyl-4-formyl-1-phenylpyrazol-5-one (2 mmol) was dissolved on stirring and heating (50–60°C) in 96% ethanol (25 mL). The corresponding hydrazide (2 mmol) was added to the obtained solution. A precipitate was formed with further stirring on heating for 1–2 h, and ethanol (10 mL), $Zn(OAc)_2 \cdot 2H_2O$ (2 mmol), and pyridine (5 mL) were added to the precipitate. The reaction mixture was stirred on heating with a reflux condenser for 4 h. The formed precipitate was left to stay overnight above the mother liquor and then was filtered off, washed with ethanol, and dried in air. Complexes **VII–XII** were obtained.

Complex $[Zn(L^1)(CH_3COO)Py]$ (**VII**), pyridineacetato-*N*′-[3-methyl-5-oxy-1-phenylpyrazol-4-yl)methylene]benzohydrazidozinc, was formed as cream-colored crystals in a yield of 85%. IR (ν, cm^{-1}): 1595 (Amide-I), 1546 (COO^-), 1530 (C=N), 1341 (COO^-), 1339 (C_{pyr}–O).

For $C_{25}H_{23}N_5O_4Zn$

Anal. calcd., %	C, 57.47	H, 4.41	N, 13.41
Found, %	C, 57.33	H, 4.29	N, 13.45

Complex $[Zn(L^2)(CH_3COO)Py]$ (**VIII**), pyridineacetato-*N*′-(3-methyl-5-oxy-1-phenylpyrazol-4-yl)methylene]-4-methylbenzohydrazidozinc, was formed as light yellow crystals in a yield of 81%. IR (ν, cm^{-1}): 1596 (Amide-I), 1557 (COO^-), 1527 (C=N), 1356 (COO^-), 1343 (C_{pyr}–O).

For $C_{26}H_{25}N_5O_4Zn$

Anal. calcd., %	C, 58.21	H, 4.66	N, 13.06
Found, %	C, 58.17	H, 4.91	N, 12.98

Complex $[Zn(L^3)(CH_3COO)Py]$ (**IX**), pyridineacetato-*N*′-(3-methyl-5-oxy-1-phenylpyrazol-4-yl)methylene]-4-methoxybenzohydrazidozinc, was formed as light yellow crystals in a yield of 90%. IR (ν, cm^{-1}): 1598 (Amide-I), 1566 (COO^-), 1530 (C=N), 1357 (COO^-), 1341 (C_{pyr}–O).

For $C_{26}H_{25}N_5O_5Zn$

Anal. calcd., %	C, 56.52	H, 4.53	N, 12.68
Found, %	C, 56.64	H, 4.60	N, 12.73

Complex $[Zn(L^4)(CH_3COO)Py]$ (**X**), pyridineacetato-*N*′-(3-methyl-5-oxy-1-phenylpyrazol-4-yl)methylene]-4-chlorobenzohydrazidozinc, was formed as light yellow crystals in a yield of 83%. IR (ν, cm^{-1}): 1601 (Amide-I), 1564 (COO^-), 1528 (C=N), 1358 (COO^-), 1341 (C_{pyr}–O).

For $C_{25}H_{22}N_5O_4ClZn$

Anal. calcd., %:	C, 53.91	H, 3.95	N, 12.58
Found, %	C, 53.77	H, 4.18	N, 12.36

Complex $[Zn(L^5)(CH_3COO)Py]$ (**XI**), pyridineacetato-*N*′-(3-methyl-5-oxy-1-phenylpyrazol-4-yl)methylene]-2-phenylethanohydrazidozinc, was formed as cream-colored crystals in a yield of 70%. IR (ν, cm^{-1}): 1604 (Amide-I), 1559 (COO^-), 1530 (C=N), 1358 (COO^-), 1342 (C_{pyr}–O).

For $C_{26}H_{25}N_5O_4Zn$

Anal. calcd., %	C, 58.21	H, 4.66	N, 13.06
Found, %	C, 58.13	H, 4.90	N, 12.92

Complex $[Zn(L^6)(CH_3COO)Py]$ (**XII**), pyridineacetato-*N*′-(3-methyl-5-oxy-1-phenylpyrazol-4-yl)methylene]-3-phenylpropanohydrazidozinc, was formed as cream-colored crystals in a yield of 72%. IR (ν, cm^{-1}): 1606 (Amide-I), 1565 (COO^-), 1530 (C=N), 1351 (COO^-), 1344 (C_{pyr}–O).

For $C_{27}H_{27}N_5O_4Zn$

Anal. calcd., %	C, 58.86	H, 4.94	N, 12.71
Found, %	C, 58.74	H, 4.69	N, 12.68

IR spectra were recorded in a range of 4000–400 cm^{-1} on a Spectrum Two FT-IR spectrophotometer (PerkinElmer) using the single-reflection attenuated total internal reflection (ATR) mode. Diffuse reflectance spectra were recorded on a Cintra 4040 spectrophotometer. Thermogravimetric (TG) studies were carried out on a STA-8000 instrument in an oxygen atmosphere.

Mass spectra were detected on a Finnagan TSQ 700 instrument. The samples were dissolved in methanol. Ions were determined by scanning in the range m/z 50–1500.

Photoluminescence (PL) spectra for the solid samples and solutions in acetonitrile were recorded on a FluoroMax-4 instrument (Horiba Scientific) with a xenon lamp (150 W) at room temperature. The luminescence quantum yield was determined by the absolute method using the Quanta-φ integration sphere.

X-ray structure analysis was carried out using the equipment of the Center for Collective Use at the St. Petersburg State University. Single crystals suitable for X-ray structure analysis were obtained by the

Table 1. Selected crystallographic data and X-ray structure experimental parameters for complexes **V** and **X**

Parameter	Value	
	V	**X**
Crystal system	Triclinic	Orthorhombic
Space group	$P\bar{1}$	*Pbca*
Cell parameters:		
a, Å	9.9078(3)	22.4975(3)
b, Å	10.4391(3)	7.78610(10)
c, Å	12.1412(3)	27.3870(4)
V, Å^3	1069.96(6)	4797.32(11)
Z	2	8
ρ_{calc}, g/cm^3	1.477	1.543
μ, cm^{-1}	1.945	2.814
F(000)	492	2288
Range of θ, deg	3.835–69.998	3.2060–71.9770
Index ranges	$-12 \le h \le 12$, $-12 \le k \le 11$, $-14 \le l \le 14$	$-27 \le h \le 27$, $-8 \le k \le 9$, $-33 \le l \le 32$
Total number of reflections	9489	25065
Independent reflections	4853	4691
Number of reflections with $I \ge 2\sigma(I)$	4314	4179
Number of refined parameters	283	327
R_1 for $I \ge 2\sigma(I)$	0.0323	0.0342
wR_2 (for all data)	0.0741	0.0865
$\Delta\rho_{min}/\Delta\rho_{max}$, e Å^{-3}	−0.52/0.310	−0.37/0.438

recrystallization of the corresponding coordination compounds from ethanol. Experimental sets of reflections for complexes **V** and **XI** were obtained using a standard method [8] on a SuperNova diffractometer equipped with a HyPix-3000 detector and a monochromatic radiation source (CuK_α, λ = 1.54184 Å).

The structures were solved by a direct method and refined in the full-matrix anisotropic approximation for all non-hydrogen atoms. The positions of the hydrogen atoms were calculated geometrically and refined in the riding model. The calculations were performed using the SHELX-2014 program package [17]. The crystallographic parameters and details of X-ray structure analysis are presented in Table 1.

The full set of X-ray structural data for compounds **V** and **XI** were deposited with the Cambridge Crystallographic Data Centre (CIF files CCDC nos. 1958400 and 1958401, respectively; deposit@ccdc.cam.ac.uk or http://www.ccdc.cam.ac.uk/data_request/cif).

RESULTS AND DISCUSSION

Hydrazones HL^1–HL^6 are convenient matrices for the synthesis of stable coordination compounds. The presence of several "acidic" hydrogen atoms and the existence of several tautomeric forms of the studied ligands assume the possibility of preparing complexes of several types depending on the degree of deprotonation of hydrazones. The studies carried out in this work show that the reactions of HL^1–HL^6 with zinc acetate lead to the formation of the complexes with the singly deprotonated form of the ligands even in the presence of pyridine excess. The compositions of the compounds were determined from the elemental analysis and ESI mass spectrometry data. The elemental analysis data indicate the 1 : 1 metal to ligand ratio in the complexes. The mononuclear structures of the complexes in solutions were confirmed by the mass spectrometry data. The mass spectra of the compounds exhibit the most intense peaks corresponding to the expected molar masses of the ZnL^+ and $ZnLH_2O^+$ particles, as well as $ZnLPy^+$. Other signals in the mass spectra are characterized by a low intensity (<15%) and correspond to the products of the partial fragmentation of the complexes under the action of the ionization source and dissociation of the complexes.

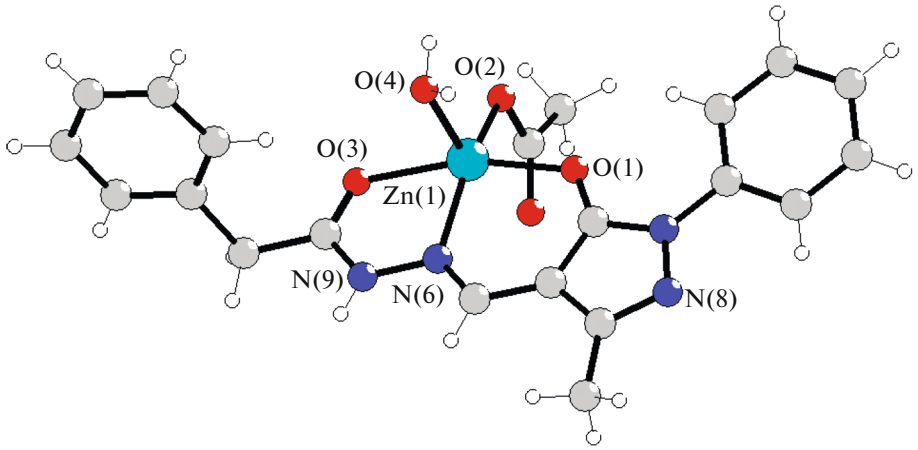

Fig. 1. Molecular structure and the enumeration of the atoms in complex **V**. Selected bond lengths: Zn(1)–O(1) 2.0393(19), Zn(1)–O(2) 1.9798(19), Zn(1)–O(3) 2.1687(19), Zn(1)–O4 2.0220(19), and Zn(1)–N6 2.048(2) Å.

The thermal stability and solvate compositions of the complexes were characterized by the TG method. According to the TG data, the complexes of both series exhibit the thermal behavior of the same type. For example, the heating of complexes **II**–**VI** to 100–180°C results in the dehydration of the complexes accompanied by an endothermic effect of ~55–65 kJ/mol indicating the coordination of the water molecule. In complex **I**, the dehydration proceeds in two stages at 60–100 and 150–190°C. Further heating results in the removal of the acetate anion and finally in the decomposition and burning out of the complex. The desolvation of complexes **VII**–**XII** proceeds in one stage in a range of 160–280°C. The mass loss corresponds to the removal of the pyridine molecule and acetate anion. The further heating leads to the complete destruction of the complexes.

The coordination mode of the acylhydrazones was determined by the IR spectroscopy data. The most indicative is the disappearance of the stretching vibration band of the C=O carbonyl group of the pyrazole fragment from the IR spectra of complexes **I**–**XII** [18]. An intense band appears instead of the latter in a range of 1339–1346 cm^{-1}, which is attributed to stretching vibrations of the $C–O^-$ group and indicates the deprotonation of the pyrazole fragment and its transformation into the enol form. The Amide-I band (1619–1632 cm^{-1}) is bathochromically shifted by 28–34 cm^{-1} compared to the spectra of the free ligands. In addition, the characteristic bands with maxima at 1566–1541 and 1361–1354 cm^{-1} are observed in the IR spectra of the complexes and are assigned to the symmetric and asymmetric stretching vibrations of the carboxyl group of the coordinated acetate anion.

The structures of coordination compounds **V** and **X** were determined using X-ray structure analysis. Complex $[Zn(L^5)(CH_3COO)H_2O]$ (**V**) crystallizes in the triclinic crystal system with the space group $P\bar{1}$. According to the X-ray structure analysis data, compound **V** has the molecular structure (Fig. 1). The coordination sphere of the zinc cation is formed by one nitrogen atom (N(6)) and oxygen atoms of the pyrazole fragment of the ligand (O(1)) and carboxyl group of hydrazone (O(3)) and by the oxygen atoms of the coordinated acetate anion (O(2)) and water (O(4)). The coordination polyhedron has the geometry of a distorted tetragonal pyramid (Addison parameter 0.19). The base of the pyramid is formed by the O(1), O(2), O(3), and N(6) atoms, and the zinc atom is raised above the pyramid base by 0.318 Å. The acetate anion is coordinated via the monodentate mode, and the acylhydrazone exists in the anionic form due to the deprotonation of the pyrazole fragment. The chelatophoric hydrazone fragment is nearly planar, and the maximum deviation from the root-mean-square plane does not exceed 0.051 Å. The phenyl ring of the benzyl radical is turned relative to the chelate fragment at an angle of 76.72°. The system of hydrogen bonds plays the key role in the formation of the crystalline lattice. The molecules of complex **V** are joined into a 3D ensemble consisting of the consequently connected centrosymmetric dimers due to the O(2)···H(4)BO(*w*4), N(8)···H(4*A*)O(*w*4), and N(9)H(9)···O(5) bonds, respectively (Fig. 2). In addition, the crystalline lattice is additionally stabilized by the system of stacking interactions between the pyrazole rings of the adjacent molecules.

Compound **X** crystallizes in the orthorhombic crystal system with the space group *Pbca* and also has the molecular structure (Fig. 3). The coordination sphere of the zinc cation is formed by two oxygen atoms and one nitrogen atom of the deprotonated hydrazone, the oxygen atom of the acetate anion, and the nitrogen atom of the coordinated pyridine molecule. The coordination mode of the pyridine molecule results in a change in the geometry of the coordination polyhedron to a distorted trigonal bipyramid (Addison

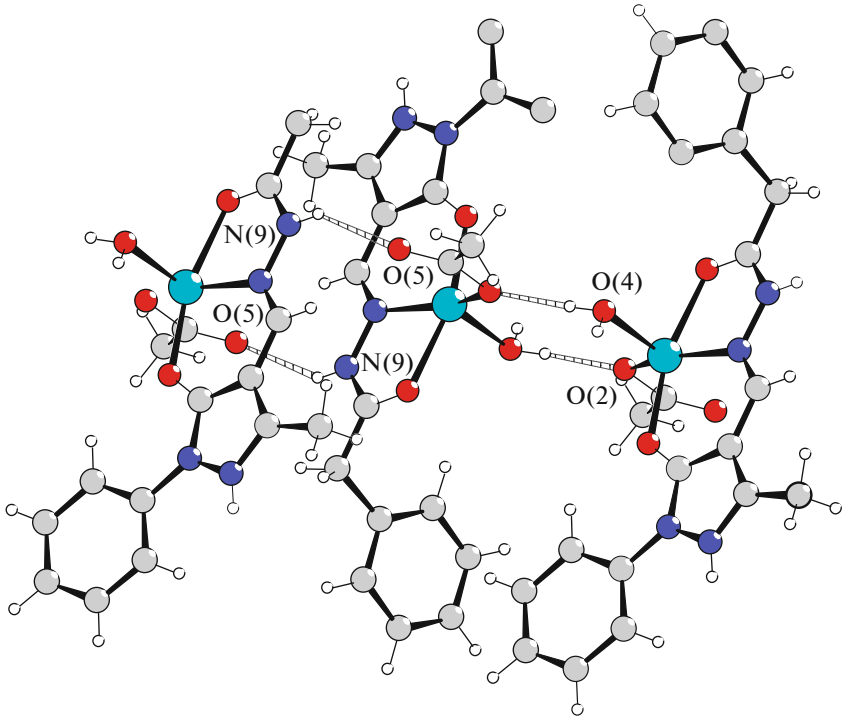

Fig. 2. Fragment of the crystal lattice of complex **V** with the hydrogen bond distribution.

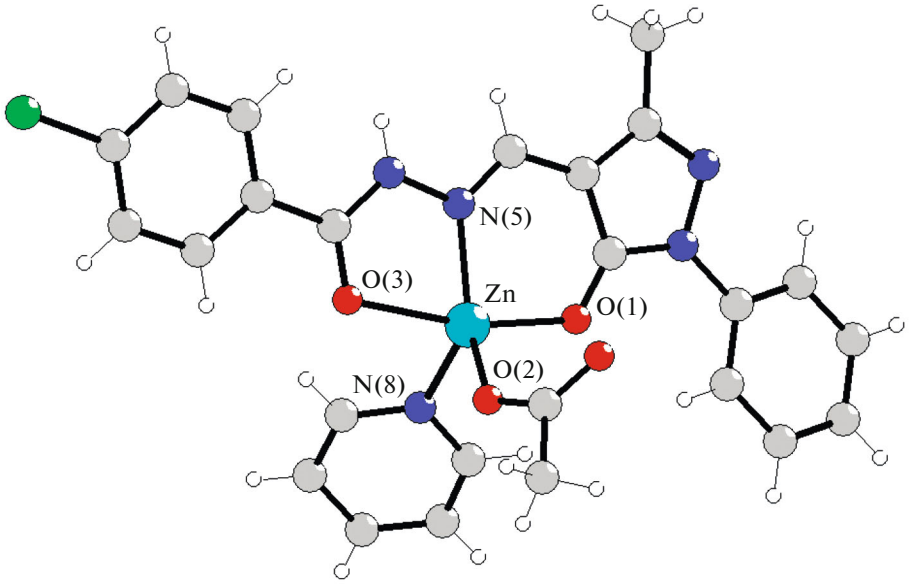

Fig. 3. Molecular structure and the enumeration of the atoms in complex **X**. Selected bond lengths: Zn–O(1) 2.0534(14), Zn–O(2) 1.9477(15), Zn–O(3) 2.2250(14), Zn–N(5) 2.0387(16), and Zn–N(8) 2.0787(16) Å.

parameter 0.57). The bond lengths in the coordination polyhedron [Zn(L^4)(CH_3COO)Py] (**X**) are close to similar parameters in complex **V**. The adjacent molecules of the complex are joined into centrosymmetric dimers due to the formation of the N(7)H(7)···O(4) hydrogen bonds.

Complexes **I**–**XII** in the solid state exhibit an intense absorbance of UV radiation with a maximum at the wavelength ~350–370 nm. For complexes **V**, **VI**, **XI**, and **XII**, the absorption maximum is shifted to the shortwave-length range compared to the complexes based on aromatic acids. The absorption is caused by

Table 2. Parameters of the luminescence spectra of the solid samples of complexes **I**–**XII**

Compound	λ_{exc}, nm	λ_{em}, nm	QY, %	CIE	τ_{Av}, ns
I	405	485	19.5	$x = 0.197$ $y = 0.319$	9.11
II	385	517	15.4	$x = 0.296$ $y = 0.568$	8.74
III	400	475	21.9	$x = 0.185$ $y = 0.306$	11.31
IV	420	495	64.2	$x = 0.186$ $y = 0.331$	12.10
V	370	425	32.9	$x = 0.157$ $y = 0.102$	9.17
VI	371	414	23.0	$x = 0.157$ $y = 0.105$	9.54
VII	395	483	30.3	$x = 0.162$ $y = 0.219$	11.9
VIII	395	536	30.0	$x = 0.388$ $y = 0.544$	15.43
IX	395	468	33.0	$x = 0.159$ $y = 0.198$	20.3
X	420	486	36.7	$x = 0.190$ $y = 0.346$	17.28
XI	373	457	27.9	$x = 0.153$ $y = 0.136$	16.17
XII	390	438	9.5	$x = 0.175$ $y = 0.199$	18.83

the electronic π–π* transitions in the conjugated system of the ligand formed by the pyrazole cycle and hydrazone fragments.

As mentioned earlier, the coordination compounds of d^{10} metals with the azomethine derivatives of salicylaldehyde are promising luminescent materials. The coordination compounds based on 4-acyl-3-methyl-1-phenylpyrazol-5-ones gain increasing significance in the recent years as more efficient photo- and electroluminophores [10, 11, 18–21], which requires the extension of the number of objects of a similar type. The qualitative checking of the luminescence properties of the synthesized coordination compounds shows that complexes **I**–**XII** in the solid state manifest an intense fluorescence in the blue, blue-green, or green ranges depending on the composition and ligand nature, whereas the fluorescence in a solution is weak (Table 2).

The initial hydrazones in the solid state exhibit a weak photoluminescence with maxima at 502 (HL^1), 520 (HL^2), 502 (HL^3), 508 (HL^4), 435 (HL^5), and 437 nm (HL^6), respectively. The luminescence intensity increases on going to the coordination compounds, and the radiation maximum is shifted to the blue range (Fig. 4), which is related to the transformation of the ligand into the different tautomeric form upon coordination.

Upon the excitation of the coordination compounds with the light with the wavelength 370–420 nm, solid complexes **I**–**VI** demonstrate an intense photoluminescence with maxima at 485, 515, 475, 493, 425, and 414 nm, respectively (Fig. 5). The broad emission bands in the PL spectra of the studied compounds are evidently caused by the energy transfer between the highest occupied and lowest unoccupied molecular orbitals. It is known that the deprotonation of organic ligands during the formation of complexes with d^{10} metals significantly decreases the energy gap between the frontier orbitals and results in the bathochromic shift of the radiation maximum in the PL spectra. The obtained data indicate that this regularity is violated. The luminescence bands of the complexes are hypsochromically shifted by 5–27 nm compared to the spectra of the corresponding free ligands. Obviously, this is related to a change in the tautomeric form of hydrazones on going to the coordination compounds [9].

The radiation maximum for the complexes based on the derivatives of aromatic acids is shifted to the red range compared to aliphatic analogs **V** and **VI**. For complexes **I**–**IV**, the maximum is regularly shifted

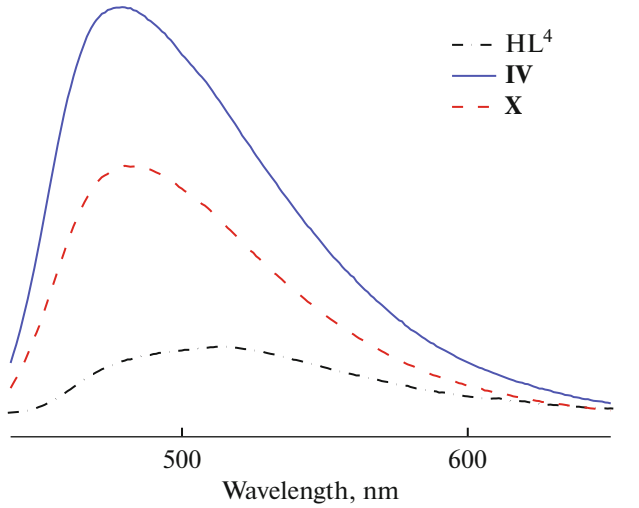

Fig. 4. Luminescence spectra of the solid samples of ligand HL^4 and complexes **IV** and **X** based on the ligand at room temperature (λ_{exc} = 380 nm).

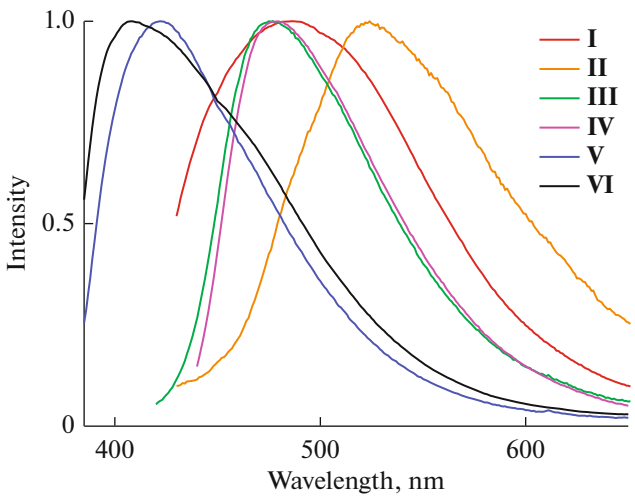

Fig. 5. Normalized luminescence spectra of the solid samples of complexes **I**–**VI** at room temperature (λ_{exc} = 380 nm).

bathochromically in the series $CH_3O < H < Cl < CH_3$, which is consistent with the enhancement of the electron-donor ability of the substituent. The introduction of methylene units into the site between the chelating unit and phenyl ring of the hydrazide fragment of the ligand shifts the luminescence maximum to the blue spectral range.

The replacement of water molecules by pyridine on going to complexes **VII**–**XII** does not basically change the shape of the luminescence spectrum. The position of the maximum is not almost changed (**VII**, **IX**, and **X**) or undergoes a bathochromic shift (**VIII**, **XI**, and **XII**) compared to that in the hydrated analogs.

Solutions of complexes **I**–**VI** in acetonitrile do not almost emit, whereas pyridine complexes **VII**–**XII** demonstrate a weak photoluminescence in the visible range with maxima at 491, 588, 470, 552, 461, and 465 nm, respectively (Fig. 6). The maxima of the spectra in the solution undergo a bathochromic shift compared to the spectra of the solid samples. This is apparently related to the decomposition of hydrogen bonds, which takes place in the crystalline lattices, and favor the electron density delocalization and bringing together the energies of the frontier orbitals.

The luminescence quantum yield of the solid samples is 9.5–64%. The PL efficiency of the hydrate complexes is lower, on the whole, than the PL efficiency of the pyridinium analogs in the case of the aromatic acid derivatives, whereas an inverse dependence is observed for the phenylalkyl derivatives. The low radiation efficiency for solutions in acetonitrile (the quantum yield is lower than 1%) is related, most likely, to the quenching effect of the OH and NH oscillators, whose action in the crystal is aligned by strong hydrogen bonds.

The lifetime of the excited state was measured for the solid samples using an analysis of the decay curves of radiation intensity quenching during monitoring of the radiation maximum. In all cases, the decay curves are well approximated by the following two-exponential functions:

$$I = A_1 \exp(\tau_1/t) + A_2 \exp(\tau_2/t), \quad (1)$$

where I is the signal intensity, A_1 and A_2 are the preexponential factors, and τ_1 and τ_2 are the lifetimes of the excited state.

The averaged lifetime τ_{Av} was calculated as follows:

$$\tau_{Av} = (A_1\tau_1 + A_2\tau_2)/(A_1 + A_2). \quad (2)$$

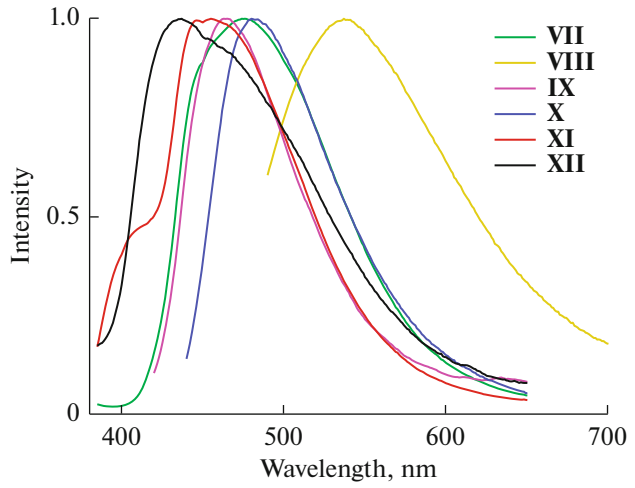

Fig. 6. Normalized luminescence spectra of the solid samples of complexes **VII**–**XII** at room temperature (λ_{exc} = 380 nm).

The general trend for the studied complexes is a shorter lifetime for complexes **I**–**VI** (8.74–12.1 ns) compared to the pyridine analogs (11.9–20.3 ns), indicating the deactivating role of the coordinated water molecules.

Thus, the influence of the substituent nature and solvate composition on the photoluminescence characteristics was examined for two series of the zinc complexes with 3-methyl-4-formyl-1-phenylpyrazol-5-one acylhydrazones. The extension of the number of objects of this type with the confirmed structures and theoretical simulation of the excited states of the molecules are needed for to understand more deeply a relationship between the structure and optical properties. Nevertheless, the studies performed show that the practical use of the synthesized coordination compounds as luminescent materials generating the blue and green emission is evidently promising.

FUNDING

This work was supported by the President of the Russian Federation in the framework of state support for young Russian scientists, doctors of science (project no. MD-1765.2019.3).

CONFLICT OF INTEREST

The authors declare that they have no conflicts of interest.

REFERENCES

1. Ch, Y. and Chou, P.-T., *Chem. Soc. Rev.*, 2010, vol. 39, p. 638.
2. Eliseeva, S.V. and Bunzl, J.-C.G., *Chem. Soc. Rev.*, 2010, vol. 39, p. 189.
3. Xu, Y., Meng, J., Meng, L., et al., *Chem.-Eur. J.*, 2010, vol. 16, p. 12898.
4. Yu, X.-Y., Ye, L., Zhang, X., et al., *Dalton Trans.*, 2010, vol. 39, p. 10617.
5. Dumur, F., Conta, E., Wantz, G., and Gigmes, D., *Eur. J. Inorg. Chem.*, 2014, p. 4186.
6. Dong, Y.-W., Fan, R.-Q., Chen, W., et al., *RSC Adv.*, 2016, vol. 6, p. 110422.
7. Li, S.M., Zheng, X.J., Yuan, D.Q., et al., *Inorg. Chem.*, 2012, vol. 51, p. 1201.
8. Dumur, F., Beouch, L., and Tehfe, M.A., et al, *Thin Solid Films*, 2014, vol. 564, p. 351.
9. Kotova, O.V., Eliseeva, S.V., Averjushkin, A.S., et al., *Russ. Chem. Bull. Int. Ed.*, 2008, vol. 57, p. 1881.
10. Gusev, A.N., Kiskin, M.A., Braga, E.V., et al., *J. Phys. Chem.*, 2019, vol. 123, p. 11850.
11. Burlov, A.S., Vlasenko, V.G., Dmitriev, A.V., et al., *Synth. Met.*, 2015, vol. 203, p. 156.
12. Xu, G.-C., Zhang, L., Zhang, Y.-H., et al., *CrystEngComm*, 2013, vol. 15, p. 2873.
13. Wang, L., Qin, W., Tang, X., et al., *J. Phys. Chem. A*, 2011, vol. 115, p. 1609.
14. Borbone, F., Caruso, U., Causa, M., et al., *Eur. J. Inorg. Chem.*, 2014, p. 2695.
15. Marchetti, F., Pettinari, C., Di Nicola, C., et al., *Coord. Chem. Rev.*, 2019, vol. 401, p. 213069.
16. Kvitko, I.Ya. and Porai-Koshits, B.A., *Zh. Org. Khim.*, 1969, vol. 5, no. 9, p. 1685.
17. Mohamed, S.K., Mague, J.T., Akkurt, M., et al., *IUCrData*, 2017, vol. 2. x171666.
18. Sheldrick, G.M., *SADABS. Program for Scanning and Correction of Area Detector Data*, Göttinngen: Univ. of Göttingen, 1997.
19. Gusev, A., Shul'gin, V., Braga, E., et al., *J. Lumin.*, 2018, vol. 202, p. 370.
20. Gusev, A.N., Shul'gin, V.F., Braga, E.V., et al., *Polyhedron*, 2018, vol. 155, p. 202.
21. Burlov, A.S., Koshchienko, Y.V., Makarova, N.I., et al., *Synth. Met.*, 2016, vol. 220, p. 543.

Translated by E. Yablonskaya